Juniper Online
Journal Material Science
ISSN: 2575-856X

Research article
Volume 7 Issue 3 - January 2023
DOI: 10.19080/JOJMS.2023.07.555714

JOJ Material Sci

P3HT: PCBM: CdSe Blends as Active Layer for Hybrid Photovoltaic Devices: Effect of TiO_2 Layers and Surface Passivation of CdSe Quantum Dots

Breno Augusto Tabosa Thome da Silva, Marco Aurelio Toledo da Silva and Sidney Alves Lourenço*

Federal Technological University of Parana, Campus Londrina, Brazil

Submitted: January 11, 2023; **Published:** January 24, 2023

***Corresponding author:** Sidney Alves Lourenço, Federal Technological University of Parana, Campus Londrina, Brazil

Abstract

In this work, hybrid photovoltaic devices with FTO/c-TiO_2/P3HT:PCBM:CdSe/Ag and FTO/c-TiO_2/mp-TiO_2/P3HT:PCBM:CdSe/Ag structures were fabricated in order to evaluate the effect of compact and mesoporous TiO_2 layers, c-TiO_2 and mp-TiO_2, as well as the outcome of cadmium selenide (CdSe) quantum dots (QDs) linked to different ligands on the performance of the cells. The CdSe QDs were synthesized via hot-injection method and passivated through solution-phase ligand exchange with three different ligands: 3-mercaptopropionic acid (MPA), thioglycolic acid (TGA) and *β*-alanine. The hybrid photovoltaic cells based on P3HT: PCBM: CdSe produced in this work presented efficiencies that varied upon the ligand anchored to the surface of the QDs; also, the cells without mp-TiO_2 presented better fill factor values than those with the layer. Finally, the implementation of CdSe QDs into the P3HT : PCBM blend reduced charge carrier recombination as could be evaluated through the shunt resistance values obtained.

Keywords: Hybrid photovoltaic devices; Quantum dots; Passivation; P3HT: PCBM: CdSe

Abbreviations: CdSe: Cadmium Selenide; QDs: Quantum Dots; MPA: 3-Mercaptopropionic Acid; TGA: Thioglycolic Acid; LUMO: Lowest Unoccupied Molecular Orbital; P3HT: Poly(3-Hexylthiophene-2,5-diyl); PCBM: Phenyl-C61-Butyric Acid Methyl Ester; QDs: Quantum Dots; ETL: Electron Transport Layer; HBL: Hole Blocking Layer; TiO2: Titanium Dioxide; HOMO: Highest Occupied Molecular Orbital

Introduction

Projected increases in world energy consumption and increasing global concern over the issue of environmental impact have focused research attention on renewable sources for power generation. Among the renewable sources, solar energy is a promising one for the clean production of electricity in the world. Solar cells are devices that are capable of converting solar energy into electrical energy through the photovoltaic effect. Along the decades, many technologies based on silicon cells have been developed to harvest sunlight and convert it into electricity. Most recently, emerging photovoltaics based on organic, inorganic, perovskite, dye-sensitized, quantum dots, among other types of cells, are being developed in search of lightweight, flexible, and low-cost manufacturing devices [1-4]. The advances in emerging photovoltaics are along with the growth in band gap engineering, which makes possible the understanding of constructing layered materials to enhance charge transport and extraction for photovoltaics; in addition, these advances accompany evolution in the field of nanoscience and nanotechnology, which includes the study of the effects of quantum confinement and surface passivation of semiconductor nanocrystals. The combination of organic and inorganic materials is another theme being studied in the search for the synergy of the best physio-chemical properties of the materials for the construction of hybrid photovoltaic cells [1,3-5].

Conductive polymers are organic materials capable of being processed into films that feature high absorption coefficient compared to films of same thickness of the inorganic counterpart; however, organic materials are not able to generate and extract charge as efficiently as inorganic materials when built into photovoltaic devices. The incorporation of inorganic materials into an organic matrix as the active layer of solar cells can benefit the performance of photovoltaic devices if the energy levels of the inorganic material are intermediate to those of the donor and acceptor, creating a cascade energy band structure. Given

the background, the material with the highest lowest unoccupied molecular orbital (LUMO) acts as donor of electrons, while the material with the lowest LUMO acts as acceptor of electrons. Poly(3-hexylthiophene-2,5-diyl) (P3HT) and Phenyl-C61-butyric acid methyl ester (PCBM) are examples of donor and acceptor materials, respectively, and they can be blended to act as the organic matrix in a hybrid solar cell. For the inorganic component, quantum dots (QDs) have grasped attention as they present band gap tunability through the quantum size effect, which allows the possibility of choosing the spectral window of the absorption profile [1,4]. The commonly used QDs are cadmium selenide (CdSe) QDs, which are usually prepared via the hot-injection method. In this context, it can be highlighted hybrid solar cells with ITO/TiO_2/P3HT:PCBM:CdSe/MoO_3/Ag and FTO/TiO_2/P3HT:PCBM:CdSe/PEDOT:PSS/Ag structures with power conversion efficiencies of 2.5% and 3.35%, respectively [3,4].

The application of QDs in solar cells requires efficient transport of charge carriers between nanocrystals, introducing electronic conductivity as a requirement for the nanocrystals' surface ligands. Typical native ligands with long hydrocarbon chains do not permit efficient electron transport. Exchanging insulating organic ligands with small molecules by surface passivation has been key to developing competitive devices [6]. By ligand exchange, new functional groups can be introduced onto the surface of the QDs, and the solubility of the nanocrystals in solvents with different polarities can be obtained [7].

In photovoltaic devices, an electron transport layer (ETL) plays a crucial role as it aids in extracting and transporting photogenerated electron carriers to the cathode of a cell; moreover, a hole blocking layer (HBL) is important to prevent that photogenerated hole carriers reaches a cell's cathode, thus avoiding a short-circuit. Titanium dioxide (TiO_2) is one of the most studied materials for these purposes due to its suitable electronic band levels and easy fabrication [8-10]. Spin coating of different titanium precursor solutions can be performed in order to obtain compact TiO_2 layer (c-TiO_2) as HBL and mesoporous TiO_2 layer (mp-TiO_2) as ETL [8,11-13].

In the present work, CdSe QDs were synthesized via hot-injection method and passivated through solution-phase ligand exchange with three different ligands: 3-mercaptopropionic acid (MPA), thioglycolic acid (TGA) and β-alanine. The CdSe QDs linked to the different ligands were implemented into P3HT:PCBM organic blends to function as active layer in hybrid photovoltaic devices. Two different structures of solar cells were fabricated to evaluate the effect of c-TiO_2 and mp-TiO_2 in the cells: FTO/c-TiO_2/P3HT: PCBM:CdSe/Ag and FTO/c-TiO_2/mp-TiO_2/P3HT:PCBM:CdSe/Ag. To characterize the materials, optical measurements were taken through UV-Vis spectrophotometry and photoluminescence spectrometry, structural investigation was accomplished via X-ray diffraction, morphological analysis was evaluated under profilometry, and electrical characterization was carried out through JxV measurements.

Experimental

Materials

Cadmium oxide (CdO, 99.5%), selenium powder (Se, ≥99.5%), trioctylphophine (TOP, 90%), 1-octadecene (ODE, 90%), 3-mercaptopropionic acid (MPA, ≥99%), thioglycolic acid (TGA, ≥98%), β-alanine (99%), methanol (≥99.9%), fluorine doped tin oxide coated glass slides (FTO, sheet resistance ~7 Ω/sq), titania paste (TiO_2 paste, particle size ~20nm), titanium(IV) isopropoxide (TTIP, 97%), and regioregular poly(3-hexylthiophene-2,5-diyl) (P3HT, M_W = 50-70 K, >90%) were all purchased from Sigma-Aldrich. Phenyl-C61-butyric acid methyl ester (PCBM, >99.5%) was acquired from SES Research. Oleic acid (OLEA) was obtained from Alphatec, toluene from Panreac, acetonitrile from Biotec, and glass slides from New Optics. Hydrogen peroxide (H_2O_2, 35%), sulfuric acid (H_2SO_4, 95-98%), acetone, and hydrochloric acid (HCl) were purchased from Anidrol. Propan-2-ol and ethanol were acquired from Dinâmica. Zinc powder (Zn) and Extran® MA 02 were obtained from Synth, and pure silver wire from Vectra. All reagents were used without further purification.

Synthesis of CdSe quantum dots

CdSe QDs were synthesized via hot-injection method following a previously reported method with few modifications [14]. In a typical synthesis, a stock solution of Se is prepared by adding 30mg of Se and 5mL of ODE into a round-bottom flask clamped over a stirrer hot plate. The flask is kept under argon flow and heated up to 100°C. Then, 0.4mL of TOP loaded in a syringe is injected to the flask with the solution under stirring. The TOP-Se solution is stored for future use. Separately, a Cd precursor solution is prepared by adding 13mg of CdO, 0.6mL of OLEA and 10mL of ODE into a three-neck round-bottom flask. The mixture in the flask is kept under stirring and argon flow, and it is heated up to 225°C; also, a reflux condenser is settled up with water flow to help with solvent volatilization. When the solution reaches 225°C, 1mL of the stored TOP-Se solution is loaded in a syringe and injected to the flask. As the Se solution is injected to the hot Cd precursor solution, the growth of CdSe QDs begins and samples of QDs with different sizes can be collected as the reaction progresses. Each sample is quenched with excess acetone in a centrifuge tube, and a small volume of toluene is added to enhance solubility. Then, the tubes are taken to centrifugation at 10,000rpm for 10 minutes. This step is repeated once; then, the supernatant is discarded and the CdSe QDs are suspended in toluene.

Surface Passivation of CdSe quantum dots

Surface passivation of the CdSe QDs was accomplished via solution-phase ligand exchange. Three ligands were employed: MPA, TGA and β-alanine. For MPA and TGA passivation's, procedures reported in the literature were carried out [15,16]. Basically, a 1μM solution of each ligand was prepared by dilution in acetonitrile. For β-alanine passivation, a different procedure was adopted [17]. Firstly, β-alanine was dissolved in ultrapure

How to cite this article: Breno A T T d S, Marco A T d S, Sidney A L. P3HT: PCBM: CdSe Blends as Active Layer for Hybrid Photovoltaic Devices: Effect of TiO_2 Layers and Surface Passivation of CdSe Quantum Dots. JOJ Material Sci. 2023; 7(3): 555714. DOI: 10.19080/JOJMS.2023.07.555714

water to get a 1M solution; then, it was further diluted in methanol to make a 1mM solution. The ligand exchange itself was performed by adding volumes of a diluted ligand solution to a 1mL CdSe QDs suspension. After every ligand addition, the suspension was stirred for half a minute and, subsequently, after stopping stirring, the suspension was allowed to stabilize for half a minute before any optical measurement was taken.

Preparation of P3HT: PCBM: CdSe blends

The experimental procedures for preparation and deposition of the P3HT: PCBM: CdSe blends was based on previously reported papers [4,18]. A total of five solutions was made. A reference solution with only P3HT:PCBM was prepared by adding 17mg of P3HT, 13mg of PCBM and 1.0mL of toluene into a vial. A P3HT:PCBM:CdSe(Oleate) solution was prepared by adding the same amount of P3HT and PCBM into a vial containing 1.0mL of as-synthesized CdSe QDs suspended in toluene. For the P3HT: PCBM: CdSe(MPA), P3HT:PCBM:CdSe(TGA) and P3HT:PCBM:CdSe(β-alanine) solutions, 1.0mL of CdSe QDs was first passivated with 100μL of a 1mM solution of the referred ligand in a vial; then, the same amount of P3HT and PCBM was added to the vials. All solutions were left at 60°C under stirring for 24h before any deposition was performed.

The glass slides used as substrates for the deposition of the solutions were cleaned by carrying out the following procedure. Firstly, the glass slides were treated in a piranha solution prepared with 35mL of H_2SO_4 and 15mL of H_2O_2 for half an hour. Next, the piranha solution was properly discarded, and the glass slides went through three steps of ultrasonic bath. The first of them in a 2% Extran® solution in distilled water for 32 minutes under heating. The second and last of them in acetone and propan-2-ol, respectively, for 8 minutes each step.

The deposition of the blends was performed by spin coating 50μL of the respective solution in two steps: initially at 500rpm for 10 seconds, and finally at 1,000 rpm for 50 seconds. After spin coating, the coated substrates were heated at 150°C for 30 minutes.

Preparation of compact and mesoporous TiO_2 layers

In order to investigate the properties of compact and mesoporous TiO_2 layers, three distinct types of samples were prepared on cleaned glass substrates: one with only compact TiO_2 layer (c-TiO_2), other with only mesoporous TiO_2 layer (mp-TiO_2) and another with both compact and mesoporous TiO_2 layers (c-TiO_2/mp-TiO_2). The methodology employed for the preparation of compact and mesoporous TiO_2 layers is reported in the literature [11-13]. It consists in preparing solutions for both c-TiO_2 and mp-TiO_2, and procedures for spin coating, drying and sintering.

For the c-TiO_2 solution, a solution of 35μL of HCl in 2.53mL of propan-2-ol was prepared ahead of a solution of 369μL of TTIP also in 2.53mL of propan-2-ol. Then, the HCl solution was added to the TTIP solution dropwise under stirring. The resulting solution was kept under stirring for at least one hour before any deposition was performed. For the mp-TiO_2 solution, a 150mg/mL solution of TiO_2 in ethanol was prepared under stirring.

The samples with only c-TiO_2 were prepared by spin coating 100μL of c-TiO_2 solution in two steps: initially at 1,500rpm for 15 seconds, and finally at 3,000rpm for 15 seconds. After spin coating, the coated substrates were dried at 120°C for 10 minutes and sintered at 500°C for 30 minutes. The substrates were allowed to cool overnight before any measurement was taken.

The samples with only mp-TiO_2 were prepared by spin coating 100μL of mp-TiO_2 solution in two steps: initially at 2,000rpm for 15 seconds, and finally at 4,000 rpm for 15 seconds. After spin coating, the coated substrate were dried and sintered with the same conditions as for the c-TiO_2. As for the c-TiO_2/mp-TiO_2 samples, the same procedures for spin coating only c-TiO_2 were first performed, then the substrates were dried at 120°C for 10 minutes; next, the same procedures for spin coating only mp-TiO2 were carried out, then the substrates were again dried at 120°C for 10 minutes. Finally, the samples were sintered at 500°C for 30 minutes and allowed to cool overnight before any measurement was taken.

Solar cell fabrication

The solar cells were fabricated in two different structures: FTO/c-TiO_2/P3HT: PCBM: CdSe/Ag and FTO/c-TiO_2/mp-TiO_2/P3HT: PCBM: CdSe/Ag in order to evaluate the performance of the photovoltaic devices with and without the incorporation of mp-TiO_2. FTO glass substrates were etched with Zn powder and HCl so that four active areas of 0.08cm^2 each were left for solar cells fabrication onto each FTO glass substrate. The substrates were cleaned following the same procedures as for the glass substrates cleaning but without treatment in piranha solution. After that, the substrates were treated in a UV chamber for 1h. Next, depending on the cell structure being developed, either only c-TiO_2 or c-TiO_2/mp-TiO_2 was deposited onto the FTO substrates following the same methodology described earlier, but leaving an area of FTO free for future cell characterization. For the active layer, 100μL of a previously prepared P3HT:PCBM:CdSe blend was spin coated in two steps: initially at 500rpm for 10 seconds, and finally at 1,000rpm for 50 seconds. After spin coating, the coated substrates were heated at 150°C for 30 minutes. For reference devices, the active layer was made with the same procedures but with a P3HT: PCBM blend without the implementation of CdSe QDs into it. Finally, four 150nm Ag electrodes were evaporated onto each device using a precision temperature controlled hi-vacuum thermal evaporating coater (MTI GSL-1700X-SPC-2) in a vacuum of 1x10-1 Pa and temperature of 1,050°C.

How to cite this article: Breno A T T d S, Marco A T d S, Sidney A L. P3HT: PCBM: CdSe Blends as Active Layer for Hybrid Photovoltaic Devices: Effect of TiO_2 Layers and Surface Passivation of CdSe Quantum Dots. JOJ Material Sci. 2023; 7(3): 555714. DOI: 10.19080/JOJMS.2023.07.555714

Characterizations

The optical properties of the synthesized CdSe QDs were measured by UV-Vis spectrophotometry and photoluminescence spectrometry. The surface passivation of the CdSe QDs was evaluated by photoluminescence spectrometry. UV-Vis spectrophotometry and photoluminescence spectrometry were conducted to analyze the optical properties of P3HT: PCBM and P3HT: PCBM:CdSe films. The structural properties of compact and mesoporous TiO_2 layers were investigated by X-ray diffraction, while their thickness and transmittance were analyzed by profilometry and UV-Vis spectrophotometry in the transmittance mode, respectively. The performance of the photovoltaic devices was evaluated through JxV measurements. The UV-Vis spectrophotometry was performed either with a double beam spectrophotometer (Biochrom Libra S60) or with an apparatus composed of a 60/55 W H4 lamp, a converging lens, a set of filters and a CCD spectrometer (Edmund Optics BRC112E-USB-VIS/NIR). The photoluminescence spectrometry was carried out with an apparatus composed of a class IIIB laser with emission in 405 nm and power around 300 mW, a pair of converging lenses, a set of filters and the same CCD specified before. The X-ray diffraction was conducted with a benchtop XRD (Bruker D2 PHASER). The profilometry was performed with a stylus profilometer (Bruker DektakXT). The JxV measurements were acquired using a precision source/measure unit (Keysight B2901A) and a solar simulator (Abet Technologies model 10500) equipped with an AM1.5G filter (100 mW/cm^2).

Results and Discussion

A total of four samples of CdSe QDs was synthesized for this work. Figure 1a shows the UV-Vis spectrum of each sample, while figure 1b shows the photoluminescence spectrum of each sample. The diameter of the QDs was calculated with the empirical equation given in Equation 1, where D is the diameter in nanometers and λ is the wavelength of the first excitonic absorption peak in nanometers [19].

$$D = (1.6122\times10^{-9})\lambda^4 - (2.6575\times10^{-6})\lambda^3 + (1.6242\times10^{-3})\lambda^2 - (0.4277)\lambda + (41.57) \quad (1)$$

The absorption spectra in figure 1a shows that the larger the diameter of the CdSe QDs are, the longer the wavelength at first excitonic absorption peak is. This redshift as the diameter of the QDs are larger is expected according to the effects of quantum confinement [20]. The photoluminescence spectra in figure 1b also reveals a redshift as the diameter of the QDs are larger. The absorbance and photoluminescence peaks of the CdSe QDs samples with diameter of 2.7, 3.1, 3.6, and 3.7nm were at 528 and 546, 553 and 574, 574 and 594, and 577 and 589nm, respectively. The difference between the wavelengths of absorbance peak and photoluminescence peak is known as Stokes shift. It is quite noticeable that the green curve in figure 1b presents a broad band at long wavelengths. That is due to trap states that occurs as undercoordinated atoms on the surface of the QDs often contribute with a set of electronic states with energies lying between the highest occupied molecular orbital (HOMO) and lowest unoccupied molecular orbital (LUMO) of the QDs [6,21]. Similar results can be found in the literature [14].

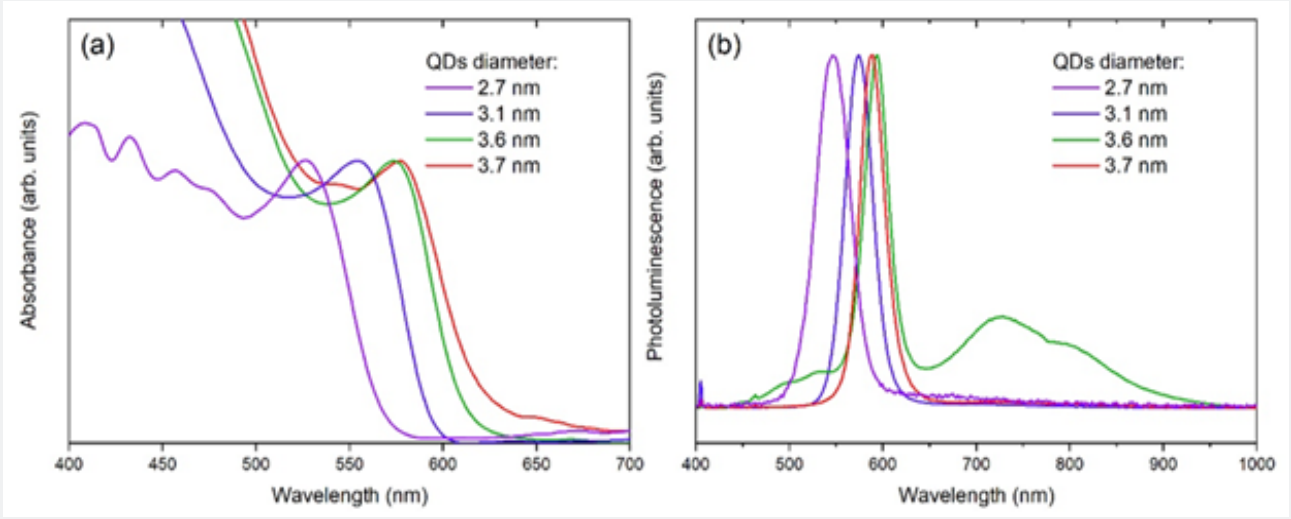

Figure 1: (a) UV-Vis and (b) photoluminescence spectra of the synthesized CdSe QDs.

The photoluminescence spectra obtained for the surface passivation of the CdSe QDs with MPA, TGA and β-alanine are shown in figure 2. Figure 2a shows that the addition of MPA to the QDs suspension causes three distinct features to arise:

a) quenching of the photoluminescence peak.

b) the intensity of the broad band related to trap states is gradually reduced.

How to cite this article: Breno A T T d S, Marco A T d S, Sidney A L. P3HT: PCBM: CdSe Blends as Active Layer for Hybrid Photovoltaic Devices: Effect of TiO_2 Layers and Surface Passivation of CdSe Quantum Dots. JOJ Material Sci. 2023; 7(3): 555714. DOI: 10.19080/JOJMS.2023.07.555714

c) the wavelength at photoluminescence peak is redshifted.

Figure 2b indicates a similar pattern for the passivation of CdSe QDs with TGA. On the other hand, figure 2c reveals that the passivation of CdSe QDs with β-alanine presents different aspects:

a) the photoluminescence peak intensifies up to a certain fraction of β-alanine in the suspension and loses intensity when the ligand is added in excess.

b) the band related to trap states is gradually weakened.

c) the wavelength at photoluminescence peak is blue shifted.

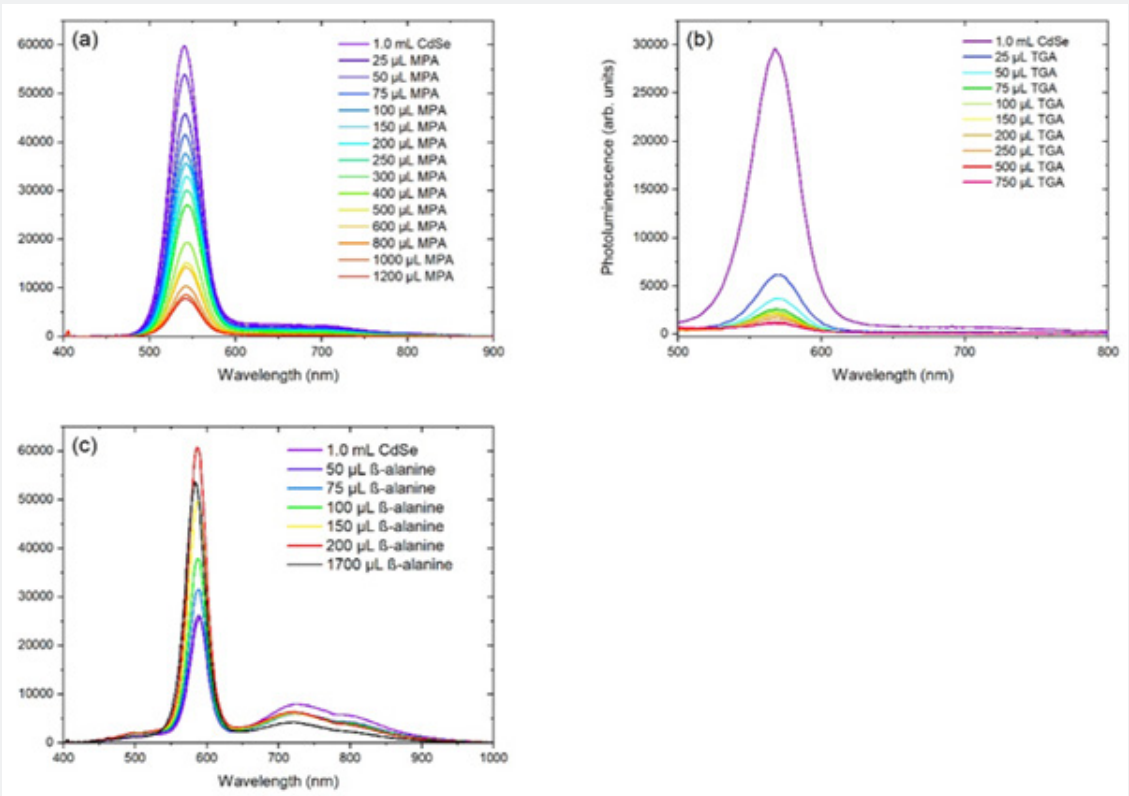

Figure 2: Photoluminescence spectra for the surface passivation of the CdSe QDs with (a) MPA, (b) TGA and (c) β-alanine.

The quenching of the photoluminescence peak for CdSe QDs passivation with MPA and TGA happens because these ligands have redox energy levels that are situated at higher energies than the QDs' HOMO; thus, hole trapping is energetically favorable and radiative recombination is strongly reduced, which results in the quenching [15,22]. The intensification of the photoluminescence peak for the QDs passivated with β-alanine is due to the ligand's nature in filling intrinsic trap states on the QDs' surface, which leads to the photoluminescence peak intensification up to a certain concentration of the ligand; however, when the ligand is added in excess, hole trapping becomes more prominent, and the photoluminescence peak reduces in intensity [17]. The band related to trap states is gradually weakened for passivation with any of the three ligands employed in this work because a strong covalent bond is formed between the QDs' surface atoms and the ligands, which shifts the energies related to trap states outside the band gap, cleaning it from fast non-radiative recombination [6]. The wavelength at photoluminescence peak is redshifted when passivating CdSe QDs with thiols, like MPA, because these ligands induces electron traps that delocalize the electronic wave function to the QDs' surface, this translates to a smaller effective QD size, which is seen as a redshift in photoluminescence spectra; contrarily, the wavelength at photoluminescence peak is blue shifted when passivating CdSe QDs with amines, like b-alanine, because these ligands confine the electronic wave function to the QDs core through Coulombic repulsive forces as the surface of the QDs becomes negatively charged, this translates to a larger effective QD size, which is seen as a blueshift in photoluminescence spectra [17]. All these features observed through photoluminescence spectrometry proves that the CdSe QDs were effectively passivated with the ligands employed in this work.

How to cite this article: Breno A T T d S, Marco A T d S, Sidney A L. P3HT: PCBM: CdSe Blends as Active Layer for Hybrid Photovoltaic Devices: Effect of TiO_2 Layers and Surface Passivation of CdSe Quantum Dots. JOJ Material Sci. 2023; 7(3): 555714. DOI: 10.19080/JOJMS.2023.07.555714

The optical characterization via UV-Vis spectrophotometry and photoluminescence spectrometry of the P3HT:PCBM and P3HT:PCBM:CdSe films resulted in the spectra presented in figure 3. The P3HT:PCBM:CdSe solutions were prepared employing the CdSe QDs with 3.7nm in diameter following the procedures described earlier.

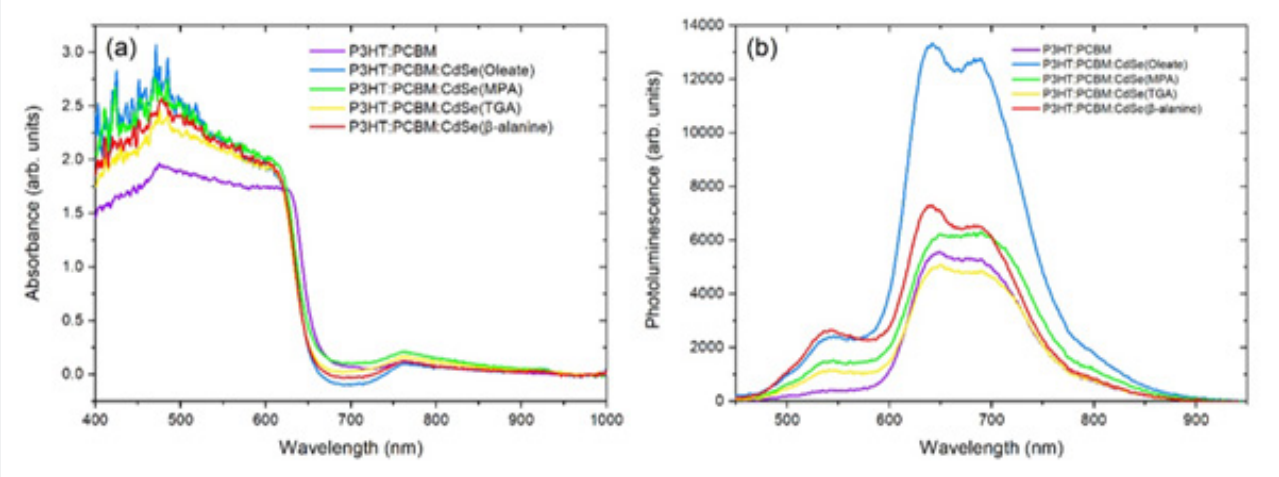

Figure 3: (a) UV-Vis and (b) photoluminescence spectra of the P3HT:PCBM and P3HT:PCBM:CdSe films.

The purple curves in figure 3a & figure 3b are related to the absorbance and photoluminescence spectra of a P3HT: PCBM single layer, respectively, and they are equivalent to the ones presented by Zakhidov et al. [23]. According to the authors, the band present between 450 and 650nm in the purple curve in figure 3a is an overlap of three bands with intense peaks at 510, 550 and 600nm related to the P3HT with a less intense band in the region between 450 and 650 related to the PCBM; on the other hand, the band with peaks at 640 and 690nm in the purple curve in figure 3b is an overlap of a band with intense peaks at 640 and 690nm related to the P3HT with a less intense peak at 710nm related to the PCBM.

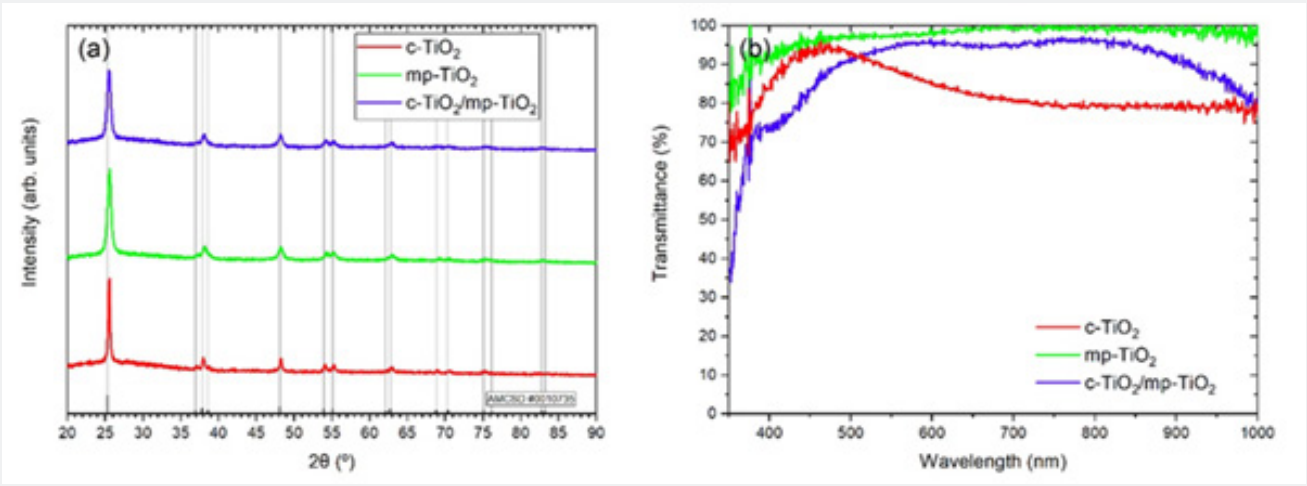

Figure 4: (a) X-ray diffractograms and (b) transmittance spectra of compact and mesoporous TiO2 layers.

The P3HT:PCBM:CdSe blends modified the reference's absorbance spectrum related to the blend without the QDs. It can be seen in Fig. 3a that the absorbances of the blends with the CdSe QDs anchored to the different types of ligands are higher compared to the reference's one; in addition, it is possible to notice an overlap of the bands related to the P3HT:PCBM blend

How to cite this article: Breno A T T d S, Marco A T d S, Sidney A L. P3HT: PCBM: CdSe Blends as Active Layer for Hybrid Photovoltaic Devices: Effect of TiO_2 Layers and Surface Passivation of CdSe Quantum Dots. JOJ Material Sci. 2023; 7(3): 555714. DOI: 10.19080/JOJMS.2023.07.555714

with the absorbance peak at 577nm related to the CdSe QDs. The refence's photoluminescence spectrum was also changed with the incorporation of the CdSe QDs linked to the different ligands in the blend. It can be seen in figure 3b that the photoluminescence increased considerably with the addition of non-passivated CdSe QDs, CdSe(Oleate); on the other hand, the addition of the QDs passivated with MPA, TGA or β-alanine maintained the photoluminescence in a range close to that of the reference's. It is also noteworthy from the photoluminescence spectra that the implementation of CdSe QDs in the P3HT:PCBM blend caused a peak around 540nm to be pronounced, the result is directly related to the presence of the QDs with photoluminescence peak at 589nm in the blends.

The structural characterization of compact and mesoporous TiO_2 layers through X-ray diffraction resulted in the diffractograms shown in figure 4a, while their optical characterization through UV-Vis spectrophotometry in the transmittance mode resulted in the spectra presented in figure 4b.

Figure 4a shows the diffractograms related to c-TiO_2 (red), mp-TiO_2 (green) and c-TiO_2/mp-TiO_2 (blue) films. It is showed, for comparison purpose, the card pattern #0010735 from American Mineralogist Crystal Structure Database (AMCSD) regarding the TiO_2 anatase phase. It can be noticed that all the peaks are in agreement with the pattern. This result confirms the presence of the anatase phase for both c-TiO_2 and mp-TiO_2, as well as c-TiO_2/mp-TiO_2. It is worth mentioning that the anatase phase provides solar cells with better performances if compared with the performance of rutile-based solar cells [24]. Figure 4b indicates that the transmittance of the obtained TiO_2 layers is very high in the visible region, while the material absorbs in the UV region, this occurs because TiO_2 has a band gap of 3.2eV [25]. Since the TiO_2 layers are along the way from the substrate to the active layer in an inverted photovoltaic device, the high transmittance of the TiO_2 layers is crucial so that most of the solar radiation reaches the solar cells' active layer. The average thickness of the obtained c-TiO_2, mp-TiO_2 and c-TiO_2/mp-TiO_2 examined by profilometry measurements were 58.2±7.5, 270±8 and 338±18nm, respectively. These results proves that the parameters used for the spin coating of the TiO_2 layers are propitious to obtaining both TiO_2 layers with adequate thickness for application in photovoltaic devices [9,26].

The JxV measurements of the FTO/c-TiO_2/P3HT:PCBM:CdSe/Ag and FTO/c-TiO_2/mp-TiO_2/P3HT:PCBM:CdSe/Ag solar cells are shown in figure 5a & figure 5b, respectively. In addition, each figure presents a black curve for the respective reference device (with only P3HT:PCBM as active layer). Figure 5c & Figure 5d present a schematic representation of the device structure for the cells with only c-TiO_2 and with both c-TiO_2 and mp-TiO_2, respectively. Figure 5e shows the energy band diagram of the FTO/TiO_2/P3HT: PCBM: CdSe/Ag solar cells with data from [3,7,25]. The P3HT: PCBM: CdSe blends used for the solar cells' active layer were prepared employing the CdSe QDs with 3.7nm in diameter.

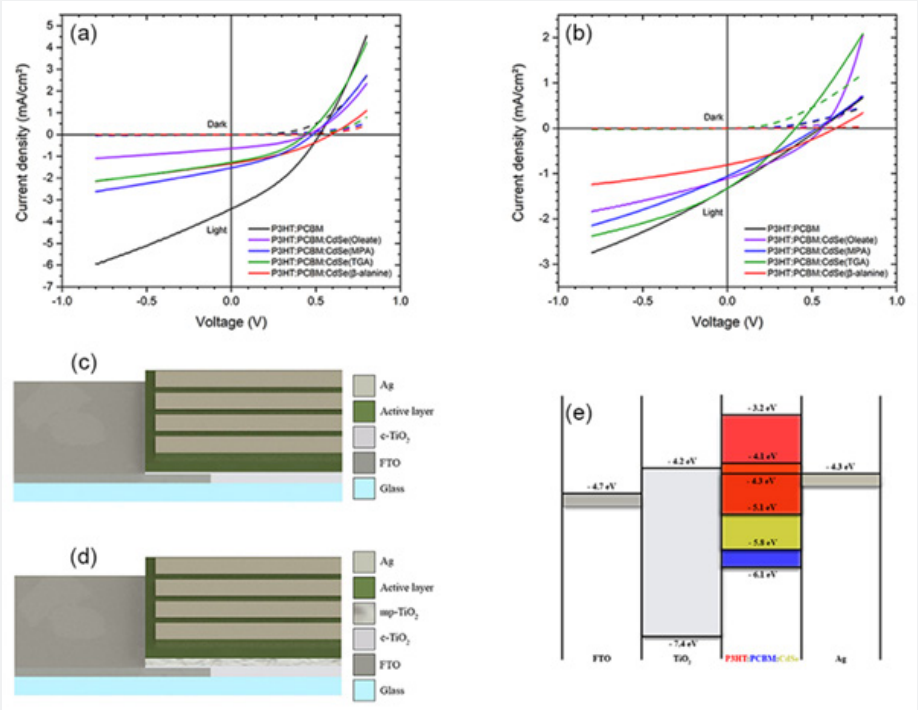

Figure 5: JxV curves of the (a) FTO/c-TiO_2/P3HT: PCBM:CdSe/Ag and (b) FTO/c-TiO_2/mp-TiO_2/P3HT:PCBM:CdSe/Ag solar cells. Schematic representation of the device structure for the (c) FTO/c-TiO_2/P3HT: PCBM:CdSe/Ag and (d) FTO/c-TiO_2/mp-TiO_2/P3HT:PCBM:CdSe/Ag solar cells. (e) Energy band scructure of the FTO/TiO2/P3HT: PCBM:CdSe/Ag solar cells.

How to cite this article: Breno A T T d S, Marco A T d S, Sidney A L. P3HT: PCBM: CdSe Blends as Active Layer for Hybrid Photovoltaic Devices: Effect of TiO_2 Layers and Surface Passivation of CdSe Quantum Dots. JOJ Material Sci. 2023; 7(3): 555714. DOI: 10.19080/JOJMS.2023.07.555714

The dashed curves were obtained for measurements of the devices under dark condition, while the solid curves were obtained for measurements under solar-simulated AM1.5G illumination (100mW/cm^2). The dashed curves indicates that all solar cells presented a rectifying diode behavior, while the solid curves demonstrates that all of them presented photovoltaic effect as the curves obtained under illumination are shifted to the fourth quadrant. Table 1 presents the acquired values for the series resistance (R_s), shunt resistance (R_{sh}), open-circuit voltage (V_{oc}), short-circuit current density (J_{sc}), fill factor (FF) and efficiency (η) of each solar cell developed. The R_s and R_{sh} values were estimated using a curve fitting methodology based on the one reported by Danielson and Depoy [27].

By comparing the η values of the solar cells with only c-TiO_2, it is noticed that all solar cells with the addition of CdSe QDs into the P3HT: PCBM blend led to a reduction in efficiency in contrast to the reference's one independent of the ligand attached to the CdSe QDs' surface (Oleate, MPA, TGA or β-alanine). Since $\eta = FF.\frac{J_{sc}.V_{oc}}{I_0}$, where I0 is the intensity of incident light (100 mW/cm^2), regardless of the increase in FF, the reduction in η is related to J_{sc} reduction, as shown in table 1. Figure 5a reveals that the P3HT: PCBM: CdSe cells have a more J-shaped JxV curve than that of the P3HT: PCBM cell, a fact that can be corroborated by the slightly higher FF values. The rise in FF means an increase in the ratio between the maximum power supplied by the cell and the cell's nominal power, which is attractive when making photovoltaic devices. This result is directly related to the increase in R_{sh} presented by the cells containing CdSe QDs into the active layer, which means that the presence of the QDs in the P3HT: PCBM blends allowed less losses due to charge carrier recombination in the cells, and this a very advantageous result. There are no report in the literature that incorporated CdSe QDs passivated with MPA, TGA or β-alanine to develop hybrid solar cells based on P3HT:PCBM:CdSe; however, there are studies that implemented CdSe QDs passivated with other ligands, such as tetrabutylammonium iodide (TBAI) [4], where the authors reached an increase in efficiency from 1.9% (without the CdSe QDs) to 2.5% for ITO/TiO_2/P3HT:PCBM:CdSe/MoO_3/Ag solar cells and, with pyridine [7], where the authors reached an efficiency of 2.96% for pyridine-passivated CdSe QDs and 2.85% for oleate-linked CdSe QDs in FTO/TiO_2/P3HT:PCBM:CdSe/PEDOT:PSS/Ag solar cells.

Table 1: Parameters attained with the electrical characterization of the solar cells developed.

Active Layer	c-TiO_2						c-TiO_2/mp-TiO_2					
	R_s (kW)	R_{sh} (kW)	V_{oc} (V)	J_{sc} (mA/cm^2)	FF	η (%)	R_s (kΩ)	R_{sh} (kΩ)	V_{oc} (V)	J_{sc} (mA/cm^2)	FF	η (%)
P3HT:PCBM	0.32	3.4	0.52	-3.4	0.34	0.62	0.60	6.3	0.55	-1.3	0.26	0.19
P3HT:PCBM:CdSe(Oleate)	1.1	19	0.45	-0.64	0.39	0.11	0.37	9.5	0.56	-1.1	0.33	0.21
P3HT:PCBM:CdSe(MPA)	0.60	9.0	0.48	-1.5	0.35	0.26	0.68	6.7	0.53	-1.1	0.27	0.15
P3HT:PCBM:CdSe(TGA)	0.60	9.7	0.44	-1.3	0.38	0.22	0.37	5.8	0.40	-1.3	0.29	0.16
P3HT:PCBM:CdSe(β-alanine)	0.95	11	0.59	-1.3	0.35	0.28	0.82	15	0.64	-0.81	0.32	0.16

The solar cells with both c-TiO_2 and mp-TiO_2 presented lower β values than their counterpart with only c-TiO_2, the only exception is for the P3HT: PCBM: CdSe (Oleate) cells. The introduction of mp-TiO_2 in addition to c-TiO_2 led to a longer path to electrons. Table 1 shows that the reference device reached an efficiency of 0.19%. For comparison, Lazim et al. [28] reached 0.21% of efficiency for ITO/TiO_2/P3HT: PCBM/Au solar cells, a value very close to the one found in this work. The insertion of oleate-linked CdSe QDs into the P3HT:PCBM blend caused the efficiency to increase to 0.21%; furthermore, the implementation caused Rs to be decreased and R_{sh} to be increased. The lower Rs indicates an enhancement in charge carrier mobility in the cells, which is an interesting result. In the literature, there are also studies that attained the same effect, Park et al. [3], for example, managed to increase the efficiency from 2.98% to 3.04% with the incorporation of tetradecylphosphinic acid linked CdSe QDs in FTO/TiO_2/P3HT: PCBM: CdSe/PEDOT: PSS/Ag solar cells. The linker in question is another surfactant molecule present in the synthesis of CdSe QDs that employs the acid instead of OLEA. Although the efficiencies of the cells with passivated QDs were lower than the reference's, figure 5b reveals that the P3HT: PCBM: CdSe cells have a more J-shaped JxV curve if compared to the highly linear P3HT: PCBM JxV curve. This result can also be corroborated by comparing the FF values in table 1; however, all c-TiO_2/mp-TiO_2 cells presented lower FF than their c-TiO_2 counterpart.

In summary, the FTO/c-TiO_2/P3HT: PCBM:CdSe/Ag cells presented better performance than the FTO/c-TiO_2/mp-TiO_2/P3HT:PCBM:CdSe/Ag cells, which indicated that the presence of mp-TiO_2 was not favorable for the cells' efficiency. This may probably be due to the greater path for charged carriers induced by the larger thickness of TiO_2 layer. The implementation of CdSe QDs into the P3HT: PCBM blend making up a hybrid solar cell reduced charge carrier recombination as could be evaluated through the R_{sh} values. This result can be associated to the incorporation of inorganic material (CdSe QDs) into an organic matrix (P3HT: PCBM), where the CdSe QDs' HOMO and LUMO are intermediate

How to cite this article: Breno A T T d S, Marco A T d S, Sidney A L. P3HT: PCBM: CdSe Blends as Active Layer for Hybrid Photovoltaic Devices: Effect of TiO_2 Layers and Surface Passivation of CdSe Quantum Dots. JOJ Material Sci. 2023; 7(3): 555714. DOI: 10.19080/JOJMS.2023.07.555714

to those of the electron donor (P3HT) and the electron acceptor (PCBM), creating a cascade energy band structure as depicted in Fig. 5e, enabling greater charge generation as well as extraction [4]. It is found in the literature for ITO/PEDOT: PSS/P3HT: PCBM: CdSe/Al [29] and FTO/TiO_2/P3HT: PCBM: CdSe/PEDOT: PSS/Ag [3] solar cells that the optimum efficiency value is obtained for low concentration of CdSe QDs. The increase in CdSe QDs concentration past a characteristic value yields to lower J_{sc} and η values. Thus, the incorporation of CdSe QDs in P3HT: PCBM for active layer in FTO/TiO2/P3HT: PCBM:CdSe/Ag solar cells can lead to an improvement in efficiency for low CdSe QDs concentration; also, highlighting, the use of only c-TiO_2 shows better results than the use of c-TiO_2/mp-TiO_2.

Conclusion

To conclude, hybrid photovoltaic devices with P3HT: PCBM: CdSe blends as active layer in FTO/TiO_2/P3HT: PCBM: CdSe/Ag solar cells were constructed and studied. The effect of both compact and mesoporous TiO_2 layers, c-TiO_2 and mp-TiO_2, as well as the response of CdSe QDs linked to oleate, MPA, TGA or β-alanine were examined on the performance of the photovoltaic devices. The synthesis of CdSe QDs through the hot-injection method resulted in QDs with diameters between 2.7 and 3.7nm with optical activity in the visible region of the spectrum. As expected, the passivation of the CdSe QDs with either MPA or TGA caused photoluminescence quenching and red shifting, while with β-alanine, the photoluminescence demonstrated to be dependent on the ligand concentration and blue shifted. Structural characterization of the TiO_2 layers indicated that both c-TiO_2 and mp-TiO_2 crystallized in the anatase phase, transmittance measurements pointed out high transmittances for both layers in the visible region, and profilometry measurements demonstrated that the thickness of c-TiO_2 and mp-TiO_2 were close to 50 and 250nm, respectively. Regarding the FTO/c-TiO_2/P3HT: PCBM: CdSe/Ag and FTO/c-TiO_2/mp-TiO_2/P3HT: PCBM: CdSe/Ag solar cells, the results indicated that the cells with only c-TiO_2 presented better performance than the cells with c-TiO_2/mp-Ti. The introduction of the mp-TiO_2 in addition to the c-TiO_2 led to a longer path to photogenerated electrons, which might be the cause of the reduction in efficiency of the overall devices based on c-TiO_2/mp-TiO_2. Even though the efficiency of the P3HT: PCBM: CdSe cells were, most of them, lower than that of the P3HT: PCBM cells, the implementation of the CdSe QDs into the P3HT: PCBM blend for the solar cells' active layer decreased charge carrier recombination as was discussed through the shunt resistance (R_{sh}) values analysis. This result is very interesting for future studies in search of improving the efficiency of hybrid solar cells.

Acknowledgement

The authors gratefully acknowledge the financial support from the following Brazilian agencies: CNPq, CAPES and Fundação Araucária. The authors would like to thank the Multiuser Laboratory of Federal Technological University of Parana - Londrina Campus - for the performed analyses.

References

1. Wright M, Uddin A (2012) Organic - inorganic hybrid solar cells: A comparative review. Sol Energy Mater Sol Cells 107: 87-111.
2. Kagan CR, Lifshitz E, Sargent EH, Talapin DV (2016) Building devices from colloidal quantum dots. Science 80: 353.
3. Park EK, Kim JH, Ji IA, Choi HM, Kim JH, et al. (2014) Optimization of CdSe quantum dot concentration in P3HT:PCBM layer for the improved performance of hybrid solar cells. Microelectron Eng 119: 169-173.
4. Nabil M, Mohamed SA, Easawi K, Obayya SSA, Negm S, et al. (2020) Surface modification of CdSe nanocrystals: Application to polymer solar cell. Curr Appl Phys 20(3): 470-476.
5. Arabpour RF, Kokabi M, Ahmadi V, Abaeiani G (2017) Structure optimization of P3HT:CdSe hybrid solar cell using optical analysis and electrochemical impedance spectroscopy. Thin Solid Films 621: 19-25.
6. Boles MA, Ling D, Hyeon T, Talapin DV (2016) The surface science of nanocrystals. Nat Mater 15(2): 141-153.
7. Park EK, Fu H, Choi M, Luan W, Kim YS (2013) Effects of ligand-exchanged cadmium selenide nanoparticles on the performance of P3HT:PCBM:CdSe ternary system solar cells. Bull Korean Chem Soc 34(8): 2321-2324.
8. Yongzhen W, Xudong Y, Han C, Kun Z, Chuanjiang Q, et al. (2014) Highly compact TiO_2 layer for efficient hole-blocking in perovskite solar cells. Appl Phys Express 7(5): 52301.
9. Lee DG, Kim CM, Kim BJ, Kim DH, Lee SM, et al. (2019) Effect of TiO_2 particle size and layer thickness on mesoscopic perovskite solar cells. Appl Surf Sci 477: 131-136.
10. Lattante S (2014) Electron and hole transport layers: Their use in inverted bulk heterojunction polymer solar cells. Electron 3: 132-164.
11. Qin J, Zhang Z, Shi W, Liu Y, Gao H, et al. (2017) The optimum titanium precursor of fabricating TiO_2 compact layer for perovskite solar cells.
12. Huang PH, Huang CW, Kang CC, Hsu CH, Lien SY, et al. (2020) The investigation for coating method of titanium dioxide layer in perovskite solar cells. Crystals 10.
13. Vivo P, Ojanperä A, Smått JH, Sandén S, Hashmi SG, et al. (2017) Influence of TiO_2 compact layer precursor on the performance of perovskite solar cells. Org Electron Physics Mater Appl 41: 287-293.
14. Boatman EM, Lisensky GC, Nordell KJ (2005) A safer, easier, faster synthesis for CdSe quantum dot nanocrystals. J Chem Educ 82(5): 1697-1699.
15. Baker DR, Kamat PV (2010) Tuning the emission of CdSe quantum dots by controlled trap enhancement, Langmuir 26(13): 11272-11276.
16. Seró IM, Giménez S, Moehl T, Fabregat SF, Lana VT, et al. (2008) Factors determining the photovoltaic performance of a CdSe quantum dot sensitized solar cell: The role of the linker molecule and of the counter electrode. Nanotechnology 19.
17. Hines DA, Kamat PV (2013) Quantum dot surface chemistry: Ligand effects and electron transfer reactions. J Phys Chem C 117: 14418-14426.
18. Dang MT, Wantz G, Bejbouji H, Urien M, Dautel OJ, et al. (2011) Polymeric solar cells based on P3HT:PCBM: Role of the casting solvent. Sol Energy Mater Sol Cells 95(12): 3408-3418.
19. Yu WW, Qu L, Guo W, Peng X (2003) Experimental determination of the extinction coefficient of CdTe, CdSe, and CdS nanocrystals. Chem Mater 15: 2854-2860.

How to cite this article: Breno A T T d S, Marco A T d S, Sidney A L. P3HT: PCBM: CdSe Blends as Active Layer for Hybrid Photovoltaic Devices: Effect of TiO_2 Layers and Surface Passivation of CdSe Quantum Dots. JOJ Material Sci. 2023; 7(3): 555714. DOI: 10.19080/JOJMS.2023.07.555714

20. Kippeny T, Swalfford LA, Rosenthal SJ (2002) Exiton in a box model. p. 79.

21. Houtepen AJ, Hens Z, Owen JS, Infante I (2017) On the Origin of Surface Traps in Colloidal II-VI Semiconductor Nanocrystals. Chem Mater 29: 752-761.

22. Wuister SF, Donegá CDM, Meijerink A (2004) Influence of thiol capping on the exciton luminescence and decay kinetics of CdTe and CdSe quantum dots. J Phys Chem B 108: 17393-17397.

23. Zakhidov E, Imomov M, Quvondikov V, Nematov S, Tajibaev I, et al. (2019) Comparative study of absorption and photoluminescent properties of organic solar cells based on P3HT:PCBM and P3HT:ITIC blends. Appl Phys A Mater Sci Process 125: 1-7.

24. Bai Y, Mora SI, De Angelis F, Bisquert J, Wang P (2014) Titanium dioxide nanomaterials for photovoltaic applications. Chem Rev 114: 10095-10130.

25. Tian J, Cao G (2013) Semiconductor quantum dot-sensitized solar cells. Nano Rev 4: 22578.

26. Zhang J, Shi C, Chen J, Wang Y, Li M (2016) Preparation of ultra-thin and high-quality WO3 compact layers and comparison of WO_3 and TiO_2 compact layer thickness in planar perovskite solar cells. J Solid State Chem 238: 223-228.

27. Danielson L, Depoy D (2006) Accurate Method for Forward and Reverse Bias Curve Fitting of TPV I-V Data.

28. Lazim HG, Ajeel KI, Badran HA (2015) The photovoltaic efficiency of the fabrication of copolymer P3HT:PCBM on different thickness nano-anatase titania as solar cell. Spectrochim Acta - Part A Mol Biomol Spectrosc 145: 598-603.

29. Ongul F, Yuksel SA, Allahverdi C, Bozar S, Kazici M, et al. (2018) Influences of CdSe NCs on the photovoltaic parameters of BHJ organic solar cells. Spectrochim Acta - Part A Mol Biomol Spectrosc 194: 50-56.

DOI: 10.19080/JOJMS.2023.07.555714

How to cite this article: Breno A T T d S, Marco A T d S, Sidney A L. P3HT: PCBM: CdSe Blends as Active Layer for Hybrid Photovoltaic Devices: Effect of TiO_2 Layers and Surface Passivation of CdSe Quantum Dots. JOJ Material Sci. 2023; 7(3): 555714. DOI: 10.19080/JOJMS.2023.07.555714